Vapour-induced phase transformation in ultrathin cellulose films

Pengfei Liu, Wei Li, Zhankui Mei, Tao Zhu, Yoshiharu Nishiyama, Howard Wang

Vapour-induced phase transformation in ultrathin cellulose films

Pengfei Liu [2,⊥], Wei Li [1,⊥], Zhankui Mei [3], Tao Zhu [2,4], Yoshiharu Nishiyama [5], Howard Wang [3,*]

[1] School of Materials Science and Engineering, Beijing Institute of Technology, Beijing 100081, China
[2] Spallation Neutron Source Science Center, Dongguan 523803, China
[3] Neutron Science Platform, Songshan Lake Materials Laboratory, Dongguan, Guangdong 523808, China
[4] Beijing National Laboratory for Condensed Matter Physics and Institute of Physics, Chinese Academy of Sciences, Beijing 100190, China
[5] Université Grenoble Alpes, CNRS, CERMAV, Grenoble 38000, France

[⊥] The authors contributed equally to this work
* Email: wangh@sslab.org.cn

Abstract

The structural transformation of thin amorphous cellulose films in water and organic solvent vapour has been studied using grazing-incidence X-ray diffraction and atomic force microscopy. Amorphous cellulose films transform to cellulose II upon exposure to water vapour, and cellulose IV_{II} in the dimethyl sulfoxide (DMSO) vapour. The anisotropy in crystalline orientation has developed during the vapour exposure, due both to the surface and confinement effects in thin film geometry. The findings imply a novel route of the vapour treatment of cellulose films to obtain unique structures.

Introduction

Cellulose materials are processed in diverse ways to obtain unique structures and properties to meet the needs of different applications. Cellulose exhibits various polymorphs in response to changes in chemical environments. Cellulose I is the allomorph found in nature and can be converted to cellulose II through processes such as regeneration or mercerization (Langan et al. 2001; Sawada et al. 2022). Similarly, treatment with liquid ammonia or a series of diamines can convert cellulose I and II to cellulose III_I and III_{II}, respectively. Thermal treatment of cellulose III_I and III_{II} in glycerol leads to the formation of cellulose IV_I and IV_{II}, respectively. (Kroon-Batenburg et al. 1996; Gardiner and Sarko 1985). However, the existence of cellulose IV_I remains controversial, primarily due to the absence of cellulose IV_I in isolated and highly crystalline states (Wada et al. 2004). On the contrary, Buleon and Chanzy prepared single crystals of cellulose IV_{II} from dilute solution of cellulose triacetate with low molecular weight by deacetylation and subsequently precipitation (Buleon and Chanzy 1979). Alternatively, hydrothermal treatment is employed as a means to augment the durability of wood (Esteves 2009; Sandberg et al. 2013). This treatment involves subjecting wood to an excessive amount of water, which results in the co-crystallization of cellulose crystallites. Consequently, a new cellulose I' allomorph is formed, bearing resemblance to cellulose IV (Kuribayashi et al. 2016). This indicates that hydrothermal treatment has the potential to induce a transformative conversion to a cellulose IV-type structure. As phase transformations among allomorphs of cellulose have been mostly studied on bulk cellulose materials in forms of powder, fibre, chip and block, investigations on structures in cellulose thin films have been limited.

Cellulose thin films are used as model systems for studying surface of cellulosic materials to elucidate fundamentals in natural or industrial settings. Potential modern applications of cellulose have expanded to technological areas such as photoresists, photoelectronics, thermoelectrics, biosensors, and tissue engineering (Kontturi and Spirk 2019; Kontturi et al. 2006; Maver et al. 2015), which demands a deeper understanding and better control of cellulose materials. Crystallization in cellulose thin films often determines their properties in adhesion (Eriksson et al. 2007), water affinity (Tammelin et al. 2015), and enzymatic hydrolysis efficiency (Hall et al. 2010), hence the applicability in related cellulose-based devices. The in-depth knowledge of structure and properties of crystalline cellulose, particularly the alignment of polymer chains in thin films and near surfaces, is essential for the reliable design and fabrication of cellulose-based devices.

The molecular arrangement of cellulose in films is affected by the presence of interfaces and the geometric confinement in the normal direction (Balko et al. 2017; Resel 2008). Crystalline lattice order of cellulose in thin films is often elusive because of the confinement and substrate interactions in different film-forming processes (Jones et al. 2019). Similarly, crystallinities and mesostructures of cellulose in thin films depend heavily on the origin of the cellulose and film preparation methods (Aulin et al. 2009). The uncertainty in the formation of cellulose films, most commonly by spin-coating solutions of cellulose or derivatives followed by cellulose regeneration and solvent removal, could vary drastically due to the biodiversity of source materials and the high sensitivity to physical conditions in the process (Kontturi et al. 2011; Lu et al. 2020; Weißl et al. 2018). Process variations could often be contained through small molecule treatment.

Manipulating interactions of cellulose with small molecules is central in the entire life cycle of processing and utilizing cellulose materials. We focus on the effect of water and dimethyl sulfoxide (DMSO). Water-induced recrystallization of amorphous cellulose to cellulose II in powders has been well characterized throughout the long history of cellulose research (Hermans and Weidinger 1946; Tyufekchiev et al. 2019), whereas those on thin film studies are recent. One example focuses on

ultrathin cellulose films, which are prepared using acid labile trimethylsilyl cellulose deposited through spin coating on silicon wafers and subsequently exposed to HCl vapour (Reishofer et al. 2022).

On the other hand, the effect of DMSO treatment on the structural ordering of cellulose is less studied. Feizi (2021) reported that partial transformation from cellulose I to II occurred when cellulose nanocrystals (CNCs) were treated with DMSO, accompanied by a significantly enhanced wettability (Feizi and Fatehi 2021). In contrast, Yang (2017) reported unchanged cellulose I crystalline structure of nanofibrillated cellulose upon DMSO soaking (Yang et al. 2017). Further studies through quantifying phase transformation in amorphous cellulose thin films upon exposure to water or DMSO will add to the collection of literatures along this line of research. Our previous studies show the reversible transformation between cellulose II and IV_{II} upon exposing the powder of near-monodisperse oligocellulose to liquid water and DMSO vapour, respectively (Zhang et al. 2021). In this study, we prepare ultrathin amorphous cellulose films and measure the evolution of cellulose structures in films upon exposing to saturated water or DMSO vapour at elevated temperatures.

Experimental

Oligocellulose was prepared using a method modified from a previous report (Jiang et al. 2021). Specifically, 6.0 g of cellulose filter paper (Cytiva) was mixed with 200 mL of 85% H_3PO_4 by mass (Shanghai Macklin Biochemical Technology Co., Ltd.). After storing in a freezer at -20 °C overnight and stirring at 60 °C for 10 hours, the mixture was slowly added to 400 mL deionized water (Merck Millipore). After filtration, the filtrate was mixed with 1200 mL methanol (Damao chemical reagent factory) and stored at room temperature overnight. The white precipitate was oligocellulose fraction DP7 with an average degree of polymerization (DP) of 7.68 and a polydispersity index (PDI) of 1.04.

DP7 was further fractionated using a previously reported method (Zhang et al. 2021). A solution of 5.0% DP7 by mass in DMSO (Sigma-Aldrich) was homogenized at 90 °C and stored at 15 °C for 3 hours. After filtering out precipitates, the solution underwent a freeze-thaw cycle between -20 °C and room temperature. The supernatant was precipitated in acetone (Xilong Scientific Co., Ltd.) 5 x by volume. The precipitates were collected through centrifugation, repeatedly washed using acetone, and dried in a vacuum oven at room temperature. The resulting oligocellulose has an average DP = 7.70 and PDI = 1.01 and is used in this study.

Molecular solutions of DP7 in anhydrous DMSO with DP7 concentrations varying from 1 to 5% by mass were homogenized at 70 °C for one hour and kept at room temperature. Thin films of DP7 were fabricated by spin-coating on a 1.5 cm × 1.5 cm silicon wafer at 2500 rpm for 90 s in a dry environment with RH < 10% and used as-cast. Cellulose film specimens were sealed in saturated vapour of water or DMSO and stored at 90 °C for 10 min before quick termination for X-ray and AFM measurements. The identical specimens were exposed to saturated vapour for an additional 20 min and subsequently measured.

The thickness of DP7 films was measured using X-ray reflectivity (XRR) on a Rigaku SmartLab diffractometer equipped with CuKα radiation. Crystalline information of the films was obtained by grazing incident X-ray diffraction (GIXRD) on the same instrument. The surface topography of DP7 films was examined using tapping mode atomic force microscopy (AFM) on a CSPM4000 instrument from Benyuan Co, Ltd. All measurements were conducted at the room temperature and in ambient atmosphere.

Results and discussion

XRR and GIXRD measurements of cellulose thin films are schematically illustrated in Figure 1a.

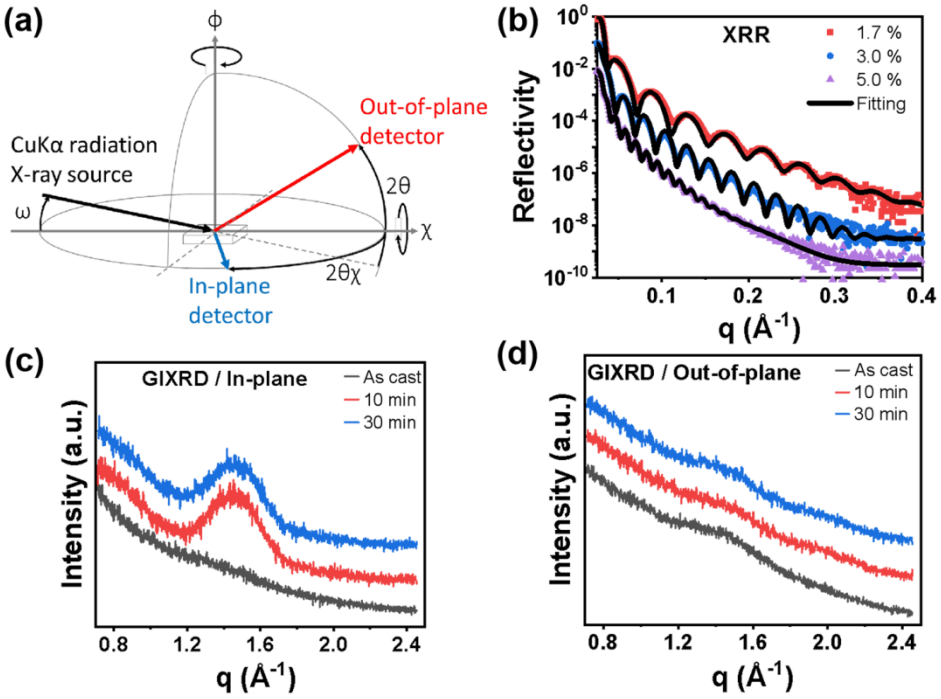

Figure 1. (a) Schematics of X-ray measurements in this study. The specimen plane is controlled by tilting angle ω, rocking angle χ, and rotating angle ϕ, and the detector can scan either in the vertical out-of-plane circle (2θ scan) or in the horizontal in-plane circle (2θχ scan). For XRR, ω and 2θ axes rotate simultaneously at a rate ratio of 1:2. In GIXRD measurements, the incident angle of the X-ray beam ω is 0.2°, slightly below the critical angle of Si, ~ 0.22°. The detector scans 2θ in the out-of-plane diffraction mode and scans 2θχ while rotating sample at ϕ = (2θχ) / 2 in the in-plane diffraction. (b) XRR of DP7 films from DP7 solutions of different concentrations in DMSO by mass. The symbols are experimental data, and curves through symbols are the best fitting using a single-layer model. XRR profiles are vertically shifted by a factor of 10 for clarity, and the thickness from the best fit is labelled correspondingly. (c) In-plane and (d) out-of-plane GIXRD of the 47 nm DP7 thin films before and after water vapour exposure for 10 and 30 min, respectively.

XRR of as cast films are shown in Figure 1b as symbols. The periodic oscillation in the specular reflectivity corresponds to the interference primarily between the X-ray waves reflected from the two interfaces of cellulose films, i.e., the air/cellulose and cellulose/substrate interfaces, respectively. The solid curves through the symbols are the best model fitting assuming a single uniform layer with a mass density of 1.50 g/cm^3. The thickness and roughness of films are 15.0 ± 0.5 nm and 0.5 ± 0.1 nm, 24.0 ± 0.2 nm and 0.7 ± 0.1 nm, and 47.0 ± 0.4 nm and 1.5 ± 0.2 nm for films cast from 1.7 %, 3.0 %, and 5.0 % solutions, respectively.

Figures 1c and 1d show as-recorded in-plane and out-of-plane GIXRD of the 47 nm DP7 films before and after exposure to water vapour. GIXRD data of films upon DMSO vapour exposure are shown in Figure S1 of the Supplementary Materials. The amorphous halo in both GIXRD profiles of the as-cast sample indicates the lack of lattice order hence the amorphous state of the as-cast films. Upon exposing to water vapour, diffraction features are prominent in in-plane geometry while rather modest in the out-of-plane GIXRD.

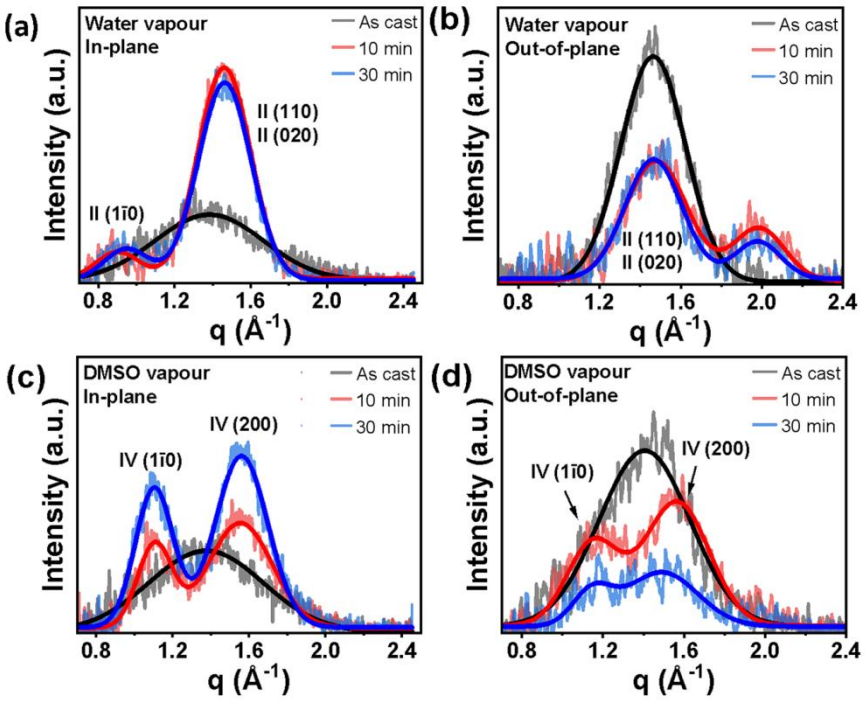

Figure 2. Background-subtracted in-plane (a, c) and out-of-plane (b, d) GIXRD of DP7 thin films before and after exposing to water (a, b) and DMSO (c, d) vapour at 90 °C for 10 and 30 min, respectively. The curves through the data are the best fit using Gaussian functions.

The diffraction features are better visualized after background subtraction and further characterized through fitting with Gaussian functions, with the best fits shown as curves through the data in Figure 2. The fitting parameters are listed in the Supplementary Materials. Figure 2a shows diffraction peaks at q = 0.9 and 1.5 Å^{-1}, which closely resembles (1$\bar{1}$0) and merged (110) and (020) of cellulose II (Langan et al. 2001; Sawada et al. 2022), respectively. It implies that saturated water vapour converts amorphous cellulose to cellulose II crystals with a unit cell containing two antiparallel chains. Longer exposure time of up to 30 min in water vapour has caused little further change to the GIXRD profiles, implying the kinetically slowing down of crystallization after 10 min. The different scattering features in Fig. 2b suggest anisotropy in crystalline structures.

In comparison, exposing thin films to DMSO vapour yields diffraction peaks at q = 1.1 and 1.6 Å^{-1}, resembling (1$\bar{1}$0) and (200) of cellulose IV$_{II}$ (Gardiner and Sarko 1985), respectively, for both in-plane (Fig. 2c) and out-of-pane diffraction (Fig. 2d), suggesting the transformation to a mostly cellulose IV phase. After additional 20 min in DMSO vapour, the in-plane diffraction intensity increases while the out-of-plane diffraction intensity decreases, indicating the continuous evolution of crystalline structures. The variations in peak location and relative intensities are likely due to the anisotropy and imperfections of crystallites formed under confinement, as illustrated below.

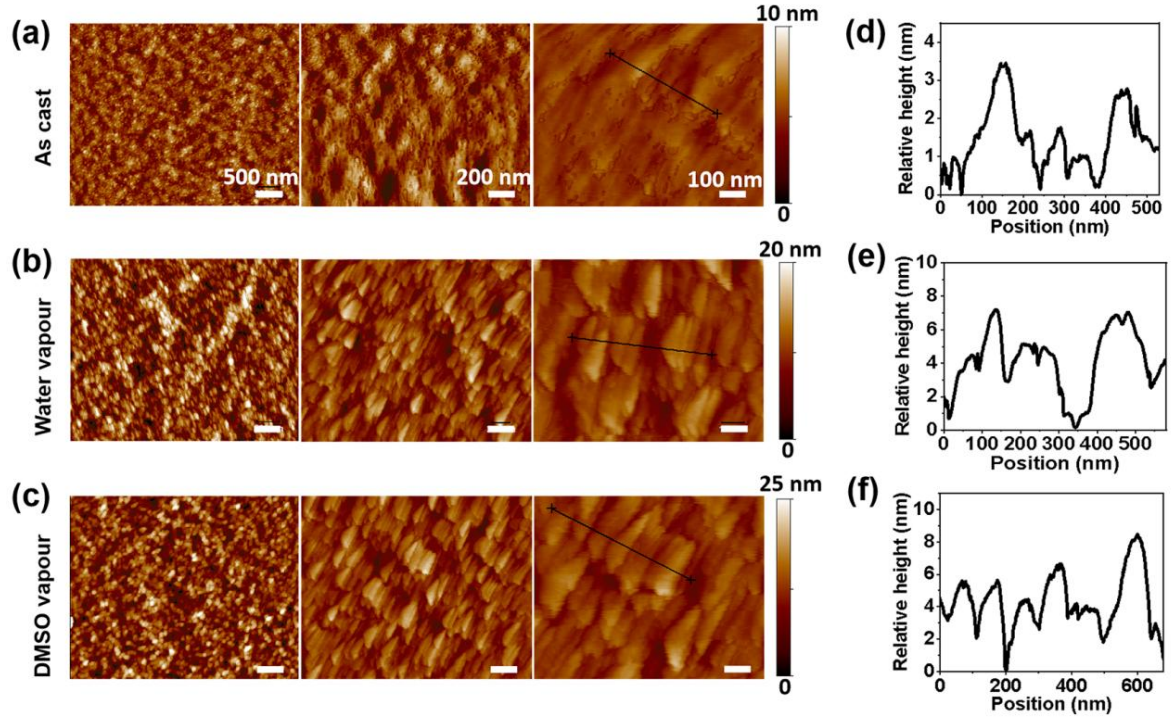

Figure 3. AFM micrographs of DP7 thin films for (a) as-cast, (b) exposed to water vapour, and (c) exposed to DMSO vapour in different magnifications, with scale bars at 500 nm (left column), 200 nm (middle column), and 100 nm (right column), respectively, with lateral dimensions from tens to hundreds of nanometres. (d) Height profiles along the black line in (a) showing features of ca.3 nm. (e, f) Height profiles along the black line in (b, c) show lamellae thickness of ca. 3 - 6 nm.

Figure 3 shows AFM micrographs of as-cast (Fig. 3a), water-treated (Fig. 3b), and DMSO-treated (Fig. 3c) DP7 films in three magnification scales. The as-cast film has a rather smooth surface of RMS roughness of 1.1 nm, due partly to somewhat regular fine features. Those after vapour treatments show significantly roughened granular surfaces with a roughness of ca. 4.0 nm. High magnification scans reveal stacks of thin platelets with lateral dimensions up to a few hundred nanometres, apparently lamellae crystallites of DP7, consistent with the diffraction data. The heights of lamellae are found from the line scans, as shown in Figs. 3e and 3f, to be in the range of 3 – 6 nm, in line with the extended-chain crystals of DP7. Given the crystal habits, it is only natural for crystallites to grow preferentially in the flat-on geometry under the confinement of the film thickness of 47 nm, i.e., the c axis along the film normal and ab plane parallel to the film surface plane.

Solvent vapour induces the phase transformation in ultrathin cellulose films to the same crystalline structure as that in the bulk oligocellulose, namely type II in water or IV_{II} in DMSO (Zhang et al. 2021). The essential differences due to the thin film geometry are in two aspects, namely the surface and confinement effects. When DP7 molecules are exposed to the vapour of polar solvents, chain ends of oligocellulose preferentially segregate to the surface, lowering the energy barrier for transforming to crystallites. On the other hand, as crystals grow larger and more perfect with the exposure time, more diffraction planes (dominantly indexed by the a, b axes) align perpendicular to the film surface due to the confinement of film thickness, consistent with the experimental data that the increase of in-plane diffraction is coupled with the decrease in out-of-plane diffraction intensity. Furthermore, the difference in diffraction features of in-plane and out-of-plane diffraction is due to the anisotropy and/or heterogeneity in the lateral dimensions. As much remain unknown in the intriguing crystallization behaviour of cellulose in thin films, detailed understanding of transformation kinetics and crystallography structures is among the topics of future studies.

Summary

Amorphous cellulose thin films have been prepared by spin-coating solutions of oligocellulose in DMSO, and subsequently exposed to water or DMSO vapour. Structures of cellulose films as-prepared and after vapour exposure have been measured using grazing-incidence X-ray diffraction and atomic force microscopy. The amorphous cellulose films transform to cellulose II upon the exposure to water vapour, and cellulose IV_{II} in DMSO. As lamellae of extended-chain crystallites develop in films during the exposure time, they orient preferably in parallel to the film plane, presumably due both to the surface and the confinement effects in the thin film geometry. The findings imply a novel route of the vapour treatment of cellulose films to obtain desirable crystalline structures and physical properties. As this preliminary work adds to the literature in better understanding cellulose films, more comprehensive studies are required to reveal details of the structural evolution and understand mechanisms of vapour-induced phase transformation in amorphous cellulose near surfaces and in confinement.

Availability of data and materials

The data that support the findings of this study are available from the corresponding author upon request.

Associated content

Supporting materials

GIXRD patterns of 5 % DP7 thin films, peak fitting parameters for GIXRD patterns of DP7 thin films.

Author information

Corresponding author

Email: wangh@sslab.org.cn, wangh@umd.edu

Competing interests

The authors declare no competing financial interest.

Authors' contributions

Z.M. produced the oligocellulose samples. P.L. prepared thin films and made the measurements. P.L. and W.L. wrote the manuscript draft. H.W. conceived the idea and edited the manuscript. H.W. and T.Z. supervised the project. All authors reviewed and revised the manuscript.

Acknowledgements

This work was supported by Beijing Institute of Technology Startup Research Fund for Young Scholars (XSQD-202108010) and Open Research Fund of Songshan Lake Materials Laboratory (2022SLABFN13).

References

Aulin C, Ahola S, Josefsson P, Nishino T, Hirose Y, Osterberg M, Wagberg L (2009) Nanoscale Cellulose Films with Different Crystallinities and Mesostructures-Their Surface Properties and Interaction with Water. Langmuir, 25(13): 7675-7685.

Balko J, Portale G, Lohwasser RH, Thelakkat M, Thurn-Albrecht T (2017) Surface induced orientation and vertically layered morphology in thin films of poly (3-hexylthiophene) crystallized from the melt. J. Mater. Res., 32(10): 1957-1968.

Buleon A, Chanzy H (1980) Single crystals of cellulose IV_{II}: preparation and properties. J. Polym. Sci., Polym. Phys. Ed., 18(6): 1209-1217.

Eriksson M, Notley SM, Wågberg L (2007) Cellulose thin films: degree of cellulose ordering and its influence on adhesion. Biomacromolecules, 8(3): 912-919.

Esteves B (2009) Wood modification by heat treatment: A review. BioResources: 370-404.

Feizi ZH, Fatehi P (2021) Changes in the molecular structure of cellulose nanocrystals upon treatment with solvents. Cellulose, 28(11): 7007-7020.

Gardiner ES, Sarko A (1985) Packing analysis of carbohydrates and polysaccharides. 16. The crystal structures of celluloses IVI and IVII. Canadian journal of chemistry, 63(1): 173-180.

Hall M, Bansal P, Lee JH, Realff MJ, Bommarius AS (2010) Cellulose crystallinity–a key predictor of the enzymatic hydrolysis rate. FEBS J., 277(6): 1571-1582.

Hermans P, Weidinger uA (1946) On the recrystallization of amorphous cellulose. J. Am. Chem. Soc., 68(12): 2547-2552.

Jiang F, Zhang X, Hwang W, Nishiyama Y, Briber RM, Wang H (2021) Oligocellulose from acid hydrolysis: A revisit. Appl. Surf. Sci., 537: 147783.

Jones AO, Resel R, Schrode B, Machado-Charry E, Röthel C, Kunert B, Salzmann I, Kontturi E, Reishofer D, Spirk S (2019) Structural Order in Cellulose Thin Films Prepared from a Trimethylsilyl Precursor. Biomacromolecules, 21(2): 653-659.

Kontturi E, Spirk S (2019) Ultrathin films of cellulose: a materials perspective. Front. Chem., 7: 488.

Kontturi E, Suchy M, Penttila P, Jean B, Pirkkalainen K, Torkkeli M, Serimaa R (2011) Amorphous characteristics of an ultrathin cellulose film. Biomacromolecules, 12(3): 770-777.

Kontturi E, Tammelin T, Österberg M (2006) Cellulose—model films and the fundamental approach. Chem. Soc. Rev., 35(12): 1287-1304.

Kroon-Batenburg L, Bouma B, Kroon J (1996) Stability of cellulose structures studied by MD simulations. Could mercerized cellulose II be parallel? Macromolecules, 29(17): 5695-5699.

Kuribayashi T, Ogawa Y, Rochas C, Matsumoto Y, Heux L, Nishiyama Y (2016) Hydrothermal transformation of wood cellulose crystals into pseudo-orthorhombic structure by cocrystallization. ACS Macro Lett., 5(6): 730-734.

Langan P, Nishiyama Y, Chanzy H (2001) X-ray structure of mercerized cellulose II at 1 Å resolution. Biomacromolecules, 2(2): 410-416.

Lu R, Zhang X, Fu L, Wang H, Briber RM, Wang H (2020) Amorphous cellulose thin films. Cellulose, 27: 2959-2965.

Maver T, Maver U, Mostegel F, Griesser T, Spirk S, Smrke DM, Stana-Kleinschek K (2015) Cellulose based thin films as a platform for drug release studies to mimick wound dressing materials. Cellulose, 22: 749-761.

Reishofer D, Resel R, Sattelkow Jr, Fischer WJ, Niegelhell K, Mohan T, Kleinschek KS, Amenitsch H, Plank H, Tammelin T (2022) Humidity Response of Cellulose Thin Films. Biomacromolecules, 23(3): 1148-1157.

Resel R (2008) Surface induced crystallographic order in sexiphenyl thin films. J. Phys.: Condens. Matter, 20(18): 184009.

Sandberg D, Haller P, Navi P (2013) Thermo-hydro and thermo-hydro-mechanical wood processing: An opportunity for future environmentally friendly wood products. Wood Mater. Sci. Eng., 8(1): 64-88.

Sawada D, Nishiyama Y, Shah R, Forsyth VT, Mossou E, O'Neill HM, Wada M, Langan P (2022) Untangling the threads of cellulose mercerization. Nature Communications, 13(1): 6189.

Tammelin T, Abburi R, Gestranius M, Laine C, Setälä H, Österberg M (2015) Correlation between cellulose thin film supramolecular structures and interactions with water. Soft Matter, 11(21): 4273-4282.

Tyufekchiev M, Kolodziejczak A, Duan P, Foston M, Schmidt-Rohr K, Timko MT (2019) Reaction engineering implications of cellulose crystallinity and water-promoted recrystallization. Green Chem., 21(20): 5541-5555.

Weißl M, Niegelhell K, Reishofer D, Zankel A, Innerlohinger J, Spirk S (2018) Homogeneous cellulose thin films by regeneration of cellulose xanthate: properties and characterization. Cellulose, 25: 711-721.

Wada M, Heux L, Sugiyama J (2004) Polymorphism of cellulose I family: reinvestigation of cellulose IVI. Biomacromolecules, 5 (4): 1385-1391.

Yang X, Wang X, Liu H, Zhao Y, Jiang S, Liu L (2017) Impact of dimethyl sulfoxide treatment on morphology and characteristics of nanofibrillated cellulose isolated from corn husks. BioResources, 12(1): 95-106.

Zhang X, Jiang F, Torres-Luna C, Nishiyama Y, Briber RM, Wang H (2021) Solvent-Assisted Fractionation of Oligomeric Cellulose and Reversible Transformation of Cellulose II and IV. ACS Biomater. Sci. Eng., 7(10): 4792-4797.